PHYSICAL REVIEW B VOLUME 35, NUMBER 4 1 FEBRUARY 1987

Band-structure calculations for Ni, Ni_4H, Ni_4H_2, Ni_4H_3, and NiH

P. Vargas*
Max-Planck-Institut für Metallforschung, Institut für Physik, 7600 Stuttgart 80, Federal Republic of Germany

N. E. Christensen
Max-Planck-Institut für Festkörperforschung,
Heisenbergstrasse 1, 7000 Stuttgart 80, Federal Republic of Germany
(Received 4 August 1986)

We present a self-consistent calculation of the electronic structure of different nickel hydrides based on the linear-muffin-tin-orbital formalism and using the local-density approximation for the exchange and correlation. The calculations for the ground state show a continuous decrease of the saturation magnetization of Ni by increasing the hydrogen concentration as a result of changes in the exchange-splitting parameter and in the Fermi energy. The presence of hydrogen in the Ni matrix modifies the electronic states of the bulk. New impurity states appearing far below from the d band of the host are found in agreement with photoemission measurements. The density of states at the Fermi level increases as a function of the hydrogen concentration, giving in this way a greater γ coefficient for the electronic specific heat than that of pure Ni. The equilibrium lattice parameter of the various Ni hydrides also increases as a function of the hydrogen concentration, reaching a saturation value for a concentration of approximately 75 at.%. All features calculated are supported by experiments, and our first-principles calculation explains the increase of the electronic specific heat together with the loss of the ferromagnetism. We also found that the electronic density around the proton occupying the octahedral sites in the fcc Ni matrix is larger than that in the free atomic hydrogen. The electron transfer occurs from the Ni atoms to the hydrogen. The polarization of H in Ni is directed opposite to the bulk polarization and of the same order of magnitude as for positive muons in the same matrix. The hyperfine field of muon in Ni can be derived by use of the calculated values for the spin density around the proton and by taking into account the zero-point motion of the positive charge around its equilibrium position.

I. INTRODUCTION

Experimental as well as theoretical studies of the electronic properties of metal-hydrogen systems have during the last decade been of great interest. One reason for this is that some of these systems are important for technological application, such as energy storage. When hydrogen is added to metals, a number of interesting modifications is produced in the metallic characteristic. The magnetic, superconducting, and mechanical properties may be dramatically changed.

When hydrogen molecules approach certain metal surfaces they dissociate due to the interaction with the surface (the dissociation energy is about 4.5 eV per molecule). This complicated process is not yet fully understood.[1] After the dissociation process the hydrogen atoms diffuse into the metal by means of hopping among interstitial sites or by means of the tunnel effect in the so-called "quantum diffusion" in which the phonons play a crucial role.[2]

In relation to the electronic structure of hydrated metals, one normally uses the adiabatic approximation in which the proton is kept frozen in an interstitial position in the bulk lattice and treated as a classical point charge, whereas the electrons are treated quantum-mechanically. This is also the approach which we use in this paper. From a structural point of view the transition from an ordered structure into a solid solution is in some metal-hydrogen systems a continuous transition and also the coexistence of various hydride phases is known to occur. Our treatment neglects these complications, and we have chosen to consider hypothetical ordered structures for the Ni-H system. This allows us to use the electronic structure method for periodic lattices. We shall study in particular the changes of the electronic states as a function of the H concentration. The calculation of the electronic states for the different ordered Ni-H systems is based on the linear-muffin-tin-orbital (LMTO) formalism,[3] and we apply the local spin-density approximation[4] for the exchange and correlation. From these calculations we derive the magnetic properties, charge transfer between H and Ni, lattice relaxations, and density-of-states (DOS) changes due to the inclusion of H atoms in the interstitial sites with octahedral symmetry in the Ni lattice. Moreover, the calculate the hyperfine field at the proton site and compare with the experimental value obtained for a muon in Ni by means of muon spin rotation (μSR) measurements.

The paper is organized as follows. In Sec. II we describe the different ordered structures calculated, and we show the results obtained for the equilibrium lattice parameter of the various Ni hydrides (including pure Ni) and the

change of volume produced by the inclusion of one H atom in the bulk. Section III gives the results achieved for the DOS of the different systems and the changes with respect to the DOS of pure Ni. The γ coefficients of the electronic specific heat are calculated and compared with available experimental data. In Sec. IV we discuss the decrease of the saturation magnetization with increasing hydrogen concentration. The spin density around the proton is obtained and used for calculating the hyperfine field at the proton position. The charge transfer between the different atomic spheres is discussed in Sec. V, and we show that charge in all systems is transferred to H from the neighboring Ni atoms. A discussion is given in Sec. VI emphasizing the following points: the volume dilatation produced by the inclusion of an H atom in transition metals, the charge transfer to hydrogen, the shape of the DOS curves and their relation to photoemission measurements, and the effect of the zero-point motion of the muon on the hyperfine field.

II. CRYSTAL STRUCTURES

In most hydrated fcc metals the hydrogen atoms are located in the interstitial sites having octahedral symmetry.[5] In the fcc lattice there is one octahedral site per bulk atom, and thus, for geometrical reasons the maximal concentration of hydrogen which can be accommodated in Ni corresponds to a NiH stoichiometry. Larger concentrations of H in Ni (NiH_x, $x>1$) reached by applying high pressure have been also reported,[6] and in these cases also a part of the interstitial sites with tetrahedral symmetry must be occupied (in an fcc host lattice there are two tetrahedral sites per atom).

Although the Ni hydrides normally form solid solutions, and also contain two phases (para- and ferromagnetic) we treat them here as ordered structures and thus we can apply the band-structure methods for crystals. Using the LMTO method[3] we introduce two types of atomic spheres, one representing the Ni atoms and the other representing the interstitial sites with octahedral symmetry. Thus even for pure Ni, there are two types of atoms: real Ni sites and so-called "empty spheres" which are formally treated as atoms without nuclear charge. In a Ni hydride we let H occupy some of the sites which in pure Ni are empty-sphere locations. Thus the structure is described as a simple-cubic Bravais lattice with a basis of eight atomic positions (see Fig. 1). By filling none, one, two, three, or four of the empty spheres representing the octahedral sites with a hydrogen atom we investigate the effect of increasing H concentration on nickel. In this manner we obtain five different stoichiometries simulating the NiH_x hydrides corresponding to $x=0$, 0.25, 0.50, 0.75, and 1, respectively.

The ratio between the radii of the overlapping atomic spheres representing the octahedral empty site (or the H atom), S_H, and the Ni atom, S_{Ni} is chosen to be

$$\frac{S_H}{S_{Ni}}=\sqrt{2}-1 . \tag{1}$$

This is the radius ratio of touching muffin-tin spheres. The overlaps between the Ni-H and Ni-Ni spheres are

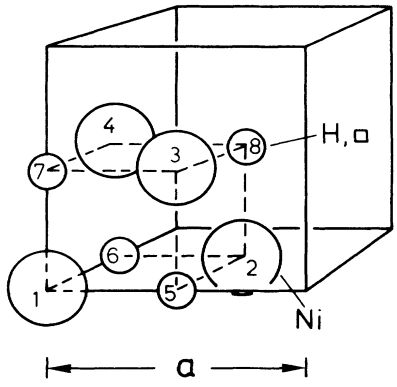

FIG. 1. Eight sphere basis used in the band-structure calculations for the Ni hydrides. The sphere radius S_H representing the H atoms (or the octahedral empty sites □) and the Ni atoms are $S_H=0.1582a$ and $S_{Ni}=0.382a$. The overlap between the Ni-H (or Ni-□) and Ni-Ni spheres are $0.04a$ and $0.057a$, respectively. The enumeration of the sites in the figure corresponds to the first column in Table II.

$0.04a$ and $0.057a$, respectively (a is the lattice parameter). The inclusion of the empty spheres in the calculation is not strictly necessary, but we have included them in order to use the same structure constants for all five Ni hydrides considered. This allows us to make comparisons between quantities which have been calculated with the same numerical accuracy. By comparing our calculation for pure Ni using the basis with eight spheres with a calculation for pure nickel using the fcc lattice with one atom per unit cell, we observe that the inclusion of empty spheres located in the octahedral sites in the calculation simulates the interstitial regions in Ni, in which the electronic density has predominantly s character. Moreover, the calculated value for the lattice parameter is in closer agreement with the experimental value than the calculated value using one atom per unit cell (see Table I), The calculation of the equilibrium lattice parameter for the different NiH_x hydrides ($x=0$, 0.25, 0.5, 0.75, 1) were made by calculating the pressure[7–9] p as a function of volume V. By interpolation the equilibrium volume V_0 is determined according to

$$p(V_0)=0 . \tag{2}$$

TABLE I. The lattice parameter for the NiH_x hydrides. The "experimental" values were obtained from Eq. (4) using the experimental value (Ref. 11) for the volume expansion $\Delta V_H=2.8$ Å^3 per added H atom in Ni.

x	a_{th} (Å)	a_{exp} (Å)
0.00	3.49	3.52
0.25	3.56	3.59
0.50	3.61	3.66
0.75	3.67	3.72
1.00	3.69	3.72

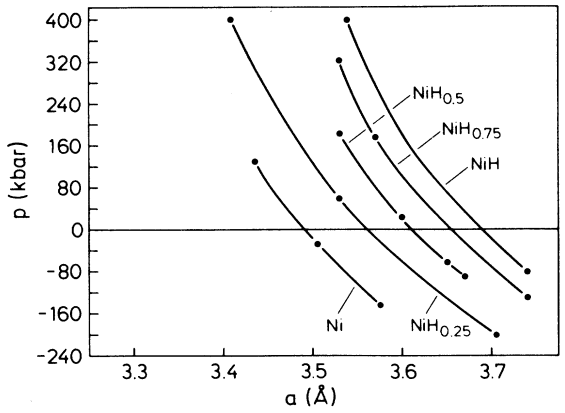

FIG. 2. Theoretical pressure—lattice-parameter curves for the different Ni hydrides examined (black dots). The equilibrium lattice parameters are the a values for which the pressure (p) vanishes.

The results for the calculated equilibrium lattice parameters are given in Table I, and the different pressure-lattice parameter curves are shown in Fig. 2.

In order to check the quality of the calculation with the inclusion of the empty spheres we have calculated the bulk modulus B for pure nickel,

$$B = -V\frac{dp}{dV}\ , \tag{3}$$

and at the experimental equilibrium volume (i.e., $a=3.52$ Å), we find the value $B=1.84$ Mbar. This is in excellent agreement with the experimental value,[10] 1.86 Mbar. The "experimental" value for the lattice parameter of the different Ni hydrides was obtained by using the experimental value for the volume expansion, ΔV_H, for H in nickel. This value[11] is $\Delta V_H = 2.8$ Å^3 per H atom. The lattice parameter for the NiH_x hydride a_{NiH_x} is then taken to be

$$a_{NiH_x} = (a_{Ni}^3 + 4x\Delta V_H)^{1/3}\ . \tag{4}$$

Here, a_{Ni} represents the lattice parameter of pure nickel ($a_{Ni}=3.52$ Å) and x the H concentration (in at.%). The relation (4) holds for H concentrations below 70 at.%. Experimentally no further change in lattice parameter is found[6] for x above 0.7. Using the theoretical results for the lattice parameter for $NiH_{0.25}$, and pure Ni in Eq. (4), we get $\Delta V_H = 2.6$ Å^3 for the volume dilatation per H atom in Ni.

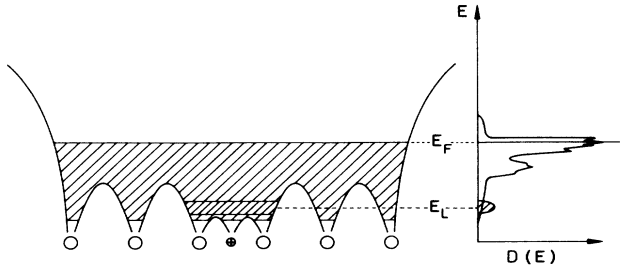

FIG. 3. Qualitative picture showing the origin of localized electronic states E_L, in the DOS curve $D(E)$, below the Fermi level E_F induced by the change of the potential due to a proton, ⊕, in an interstitial site.

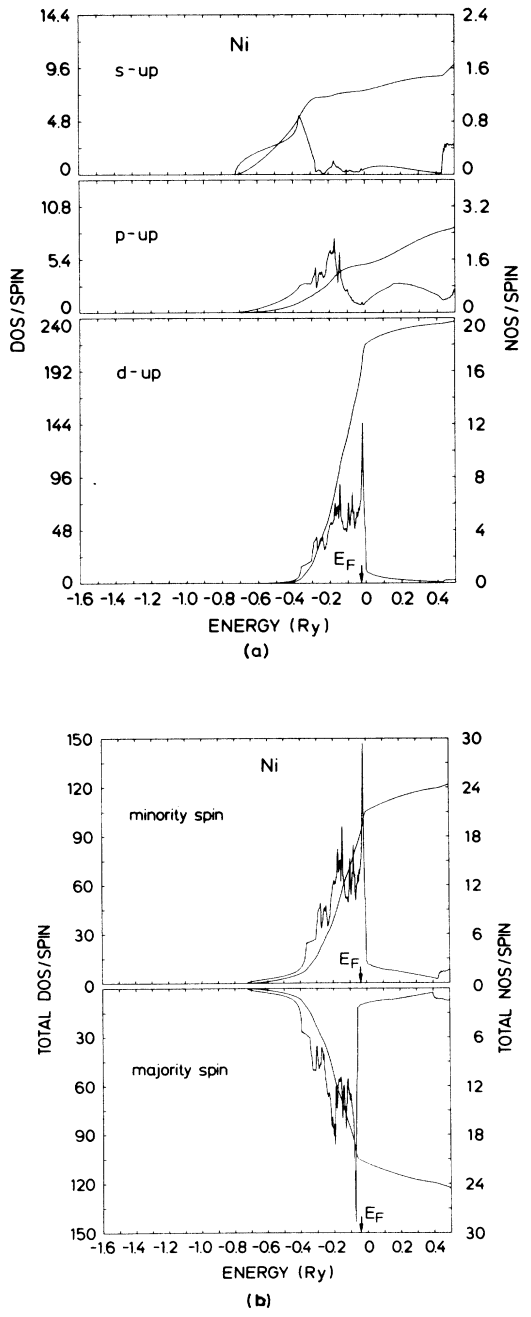

FIG. 4. Density-of-states (DOS) and number-of-states (NOS) curves for pure Ni. (a) The s, p, and d projected DOS per spin (the minority spin) on the four equivalent Ni atoms in pure nickel. [Obtained from the basis shown in Fig. 1 in which the four small interstitial spheres (5—8) are empty.] (b) The total DOS, minority spin (upper panel), and majority spin (lower panel) for pure nickel; the Fermi energy is indicated by arrows.

III. DENSITY OF STATES

One of the most important differences between the DOS functions for the Ni hydrides (see Figs. 3–9) and that of pure Ni is the appearance of structure due to new impurity states localized far below from the Fermi level. These states are mainly of s character, and arise from a strong mixing of the $1s$ state of hydrogen with the electron states of the neighboring Ni atoms. These new localized states are caused by the deepening of the effective potential seen by the electron due to the proton in the inter-

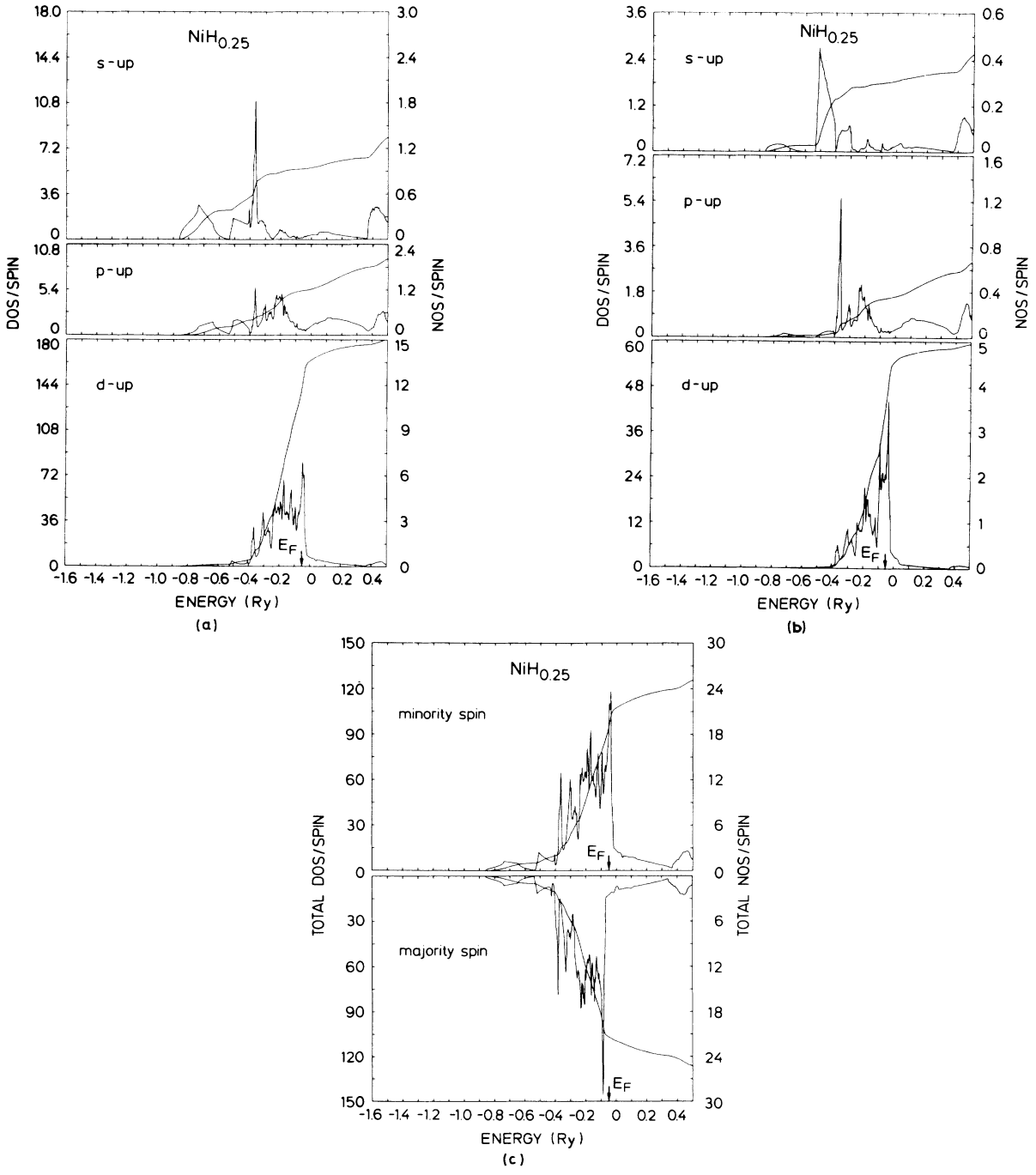

FIG. 5. DOS curves for ferromagnetic $NiH_{0.25}$; this structure is obtained by placing one H atom in the atomic sphere labeled 8 in the unit cell (see Fig. 1). (a) The s, p, and d projected DOS (minority spin) on three of the six equivalent Ni atoms closest to H. The spheres are 2, 3, and 4 in Fig. 1. (b) The s, p, and d projected DOS per spin (minority spin) on one of the eight second-nearest-neighbor Ni atoms to H (sphere 1 in Fig. 1). (c) The total DOS, minority spin (upper panel), and majority spin (lower panel) for $NiH_{0.25}$. The Fermi energy is indicated by small arrows.

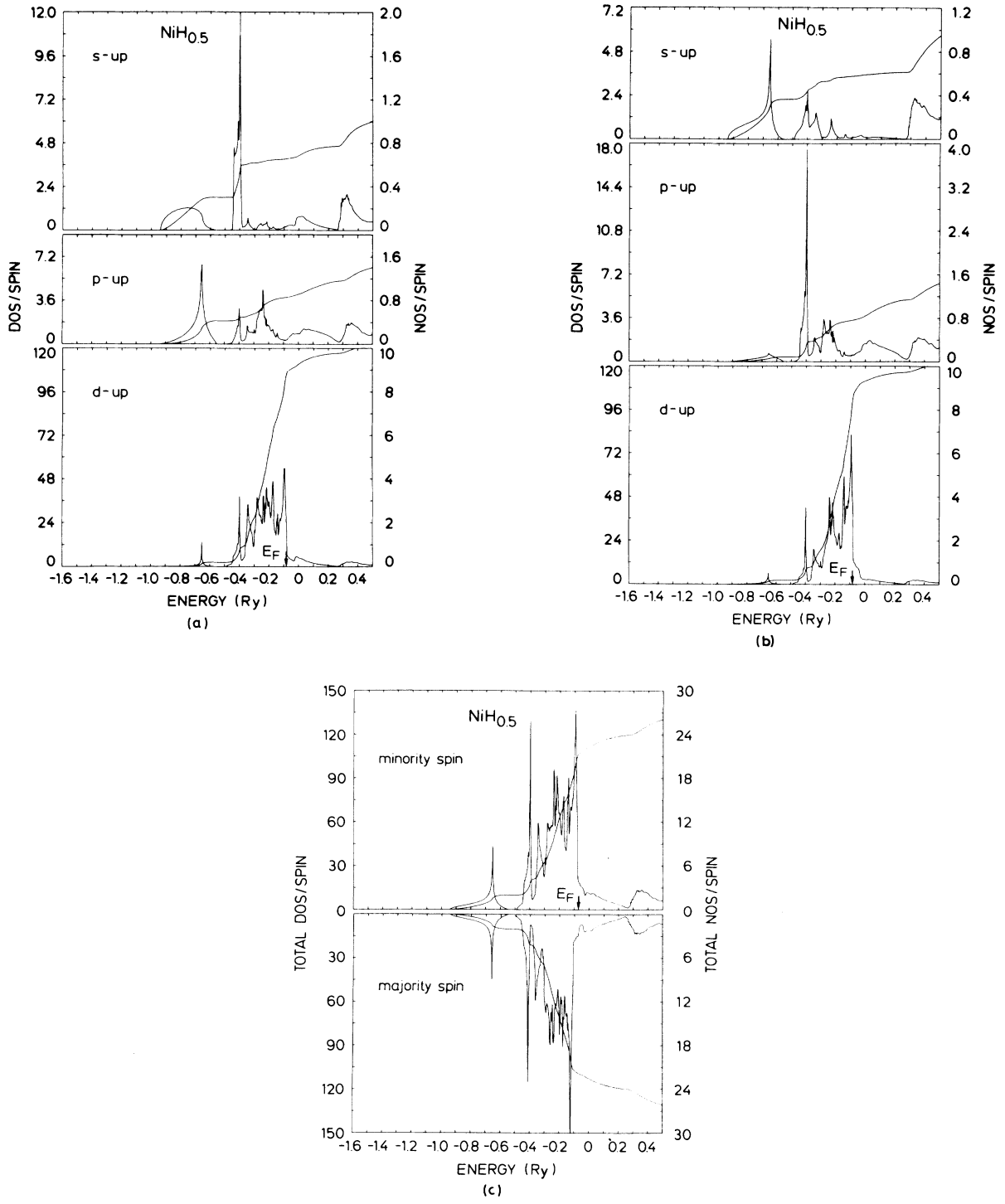

FIG. 6. DOS curves for ferromagnetic $NiH_{0.5}$. The $NiH_{0.5}$ structure is obtained by placing two H atoms in the interstitial spheres 7 and 8 in the unit cell (see Fig. 1). (a) the *s*, *p*, and *d* projected DOS per spin (minority spin) on hydrogen's two equivalent nearest-neighbor Ni atoms, spheres 3 and 4 in Fig. 1. (b) The *s*, *p*, and *d* projected DOS (minority spin) on the other two Ni spheres (1 and 2 in Fig. 1). (c) The total DOS, minority spin (upper panel), and majority spin (lower panel) for $NiH_{0.5}$. The position of the Fermi energy is indicated by arrows.

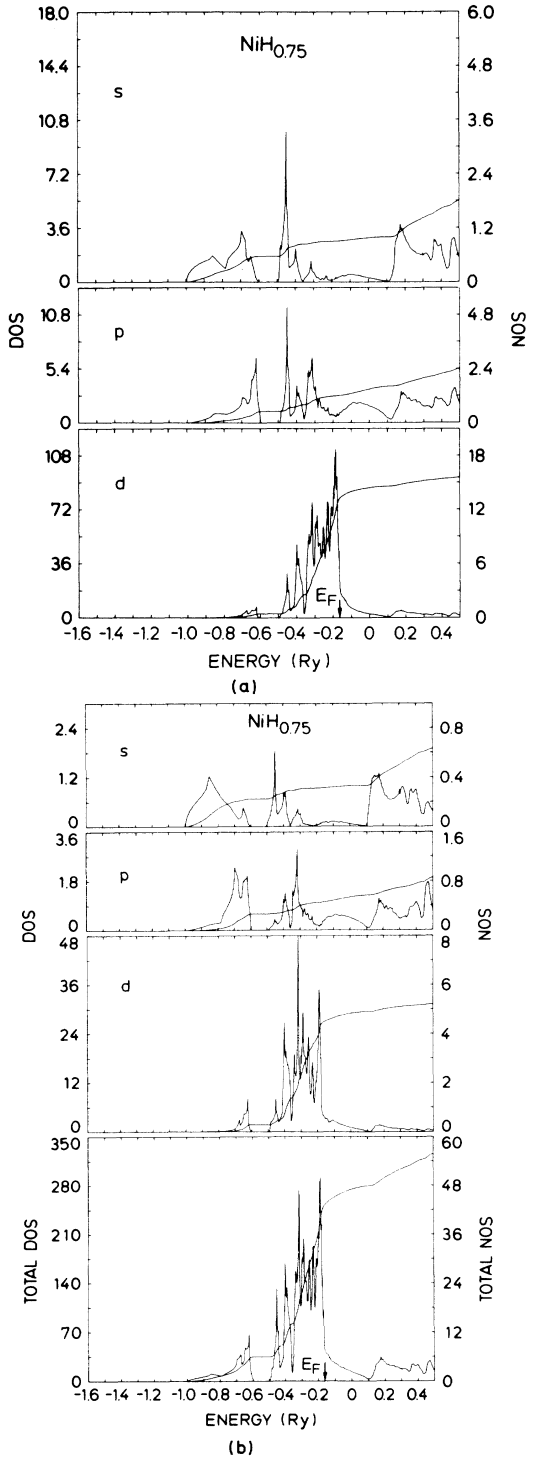

FIG. 7. DOS curves for $NiH_{0.75}$ (paramagnetic system). The structure considered is obtained by placing three H atoms in the interstitial spheres 5, 6, and 7 in Fig. 1. (a) The *s*, *p*, and *d* projected DOS on the three equivalent Ni atoms corresponding to spheres 2, 3, and 4 in Fig. 1. (b) The *s*, *p*, and *d* DOS functions shown in the upper panels are the projected DOS on the Ni atom in sphere 1 (Fig. 1). This atom is fully coordinated by six H atoms in the periodic structure. The lowest panel shows the total DOS for this paramagnetic system. The Fermi level is indicated by the arrows.

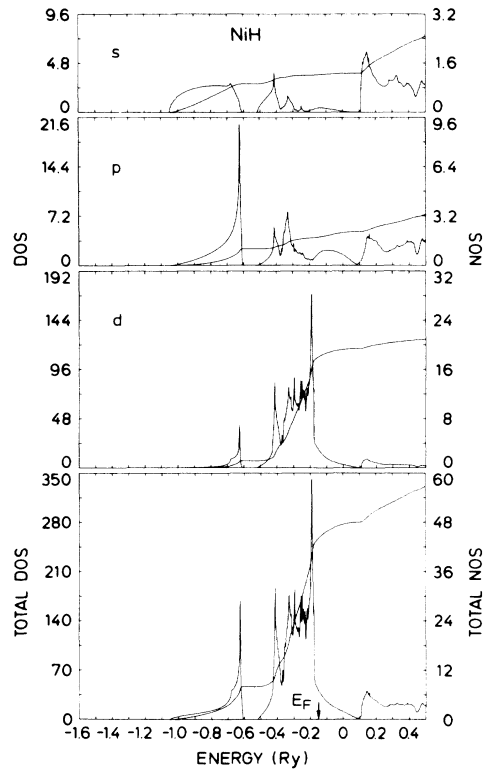

FIG. 8. DOS curves for NiH (paramagnetic). The structure is obtained by placing four H atoms in the interstitial spheres 5, 6, 7, and 8 in the unit cell (see Fig. 1). The first three upper panels show the *s*, *p*, and *d* partial DOS of the four equivalent Ni atoms (spheres 1, 2, 3, and 4 in Fig. 1). The lowest panel shows the total density of states. The Fermi energy is indicated by arrows.

stitial site as illustrated in Fig. 9. This new band with a width of ≈ 0.3 Ry is localized at 0.6 Ry below the Fermi level in all four NiH_x hydrides ($x=0.25$, 0.5, 0.75, 1.0). A small H *s* peak around 0.3 Ry below the Fermi energy appears in $NiH_{0.25}$, $NiH_{0.5}$, and $NiH_{0.75}$, but not in NiH.

The partial 4*s* DOS functions of the Ni atoms closest to the hydrogen atom exhibit for all the hydrides a gap in the occupied part of the 4*s* band. This is caused by the hybridization between the 4*s* electrons of Ni and the 1*s* electrons of the H atoms. Likewise, the 4*p* partial DOS of the Ni atoms which are nearest neighbors of the H atom exhibits a gap. This is clearly seen by comparing with the 4*p* bands of pure Ni, and it shows that there is a strong H *s*—Ni *p* hybridization. Moreover, due to the inclusion of the H atoms, there is an enhanced DOS structure due to the lower Ni 4*p* states ≈ 0.6 Ry below the Fermi energy where the *s* band of hydrogen is located. The partial DOS plots for the ferromagnetic cases (i.e., NiH_x, $x=0$, 0.25, 0.5) are given only for the minority spin since the shape of the DOS for both polarizations is very similar.

The 3*d* partial DOS of the Ni atoms closest to H shows that the lower part of the 3*d* bands is strongly affected by the presence of the hydrogen. A strong enhancement of the Ni 3*d* contribution occurs at approximately 0.6 Ry

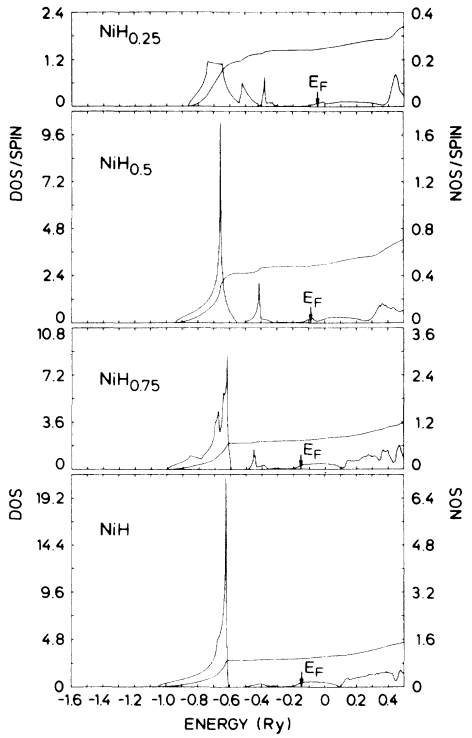

FIG. 9. H s partial DOS in the different Ni hydrides. The arrows indicate in each panel the Fermi level.

below the Fermi energy where the $3d$ DOS for pure Ni is practically negligible. There is also an enhancement of the Ni $3d$ component at 0.3 Ry below the top of the $3d$ bands. The upper part of the $3d$ bands remains practically unaltered. Since some $3d$ states are depleted from the lower region of the d band when Ni interacts with hydrogen, the $3d$ band of the Ni hydrides has a narrower width than that of pure Ni. In the case of the $NiH_{0.25}$ hydride there exists a second shell of Ni atoms around each H atom. The new $3d$ states at 0.6 Ry below the Fermi energy discussed above are for those not found, and the other corresponding enhanced electronic states are clearly reduced. This shows that the electronic redistribution caused by the presence of the hydrogen atom is very localized; in case of lower H concentration, probably the effects of the hydrogen atom are screened in the first two layers of neighboring Ni atoms.

Although the shape of the upper part of the DOS curve for the NiH_x hydrides remains practically unaltered by the presence of hydrogen in different concentrations; the DOS at the Fermi energy depends sensitively on x. Small changes in the Fermi level with respect to the value in pure Ni give rise to huge changes in the DOS at E_F. This is due to the high peak of the DOS in pure Ni at the Fermi level.

In order to make accurate comparisons for the DOS at the Fermi energy for the different hydrides at different volumes, we have used the same structure constants[3] for the various hydrides. The k-space integration used 165 k points in the irreducible part of the Brillouin zone. The calculated DOS at E_F for the different hydrides as well as for pure Ni is shown in Fig. 10(a). The results show that, at the experimental volume, the DOS at the Fermi level increases with H concentrations up to $x=0.5$. At larger concentrations of hydrogen the $3d$ bands of Ni are completely filled and the Fermi level is located above the top of the $3d$ bands, i.e., where the DOS is considerably lower. This behavior of the DOS at the Fermi level influences strongly the electronic specific heat of the Ni hydrides. Figure 10(b) shows experimental results for the γ coefficient of the electronic specific heat for different nonstoichiometric Ni hydrides. The γ coefficient is related to the DOS at the Fermi energy, $D(E_F)$, by the following relation:

$$\gamma=\tfrac{1}{3}\pi^2 k_B^2 D(E_F)(1+\lambda)\ , \tag{5}$$

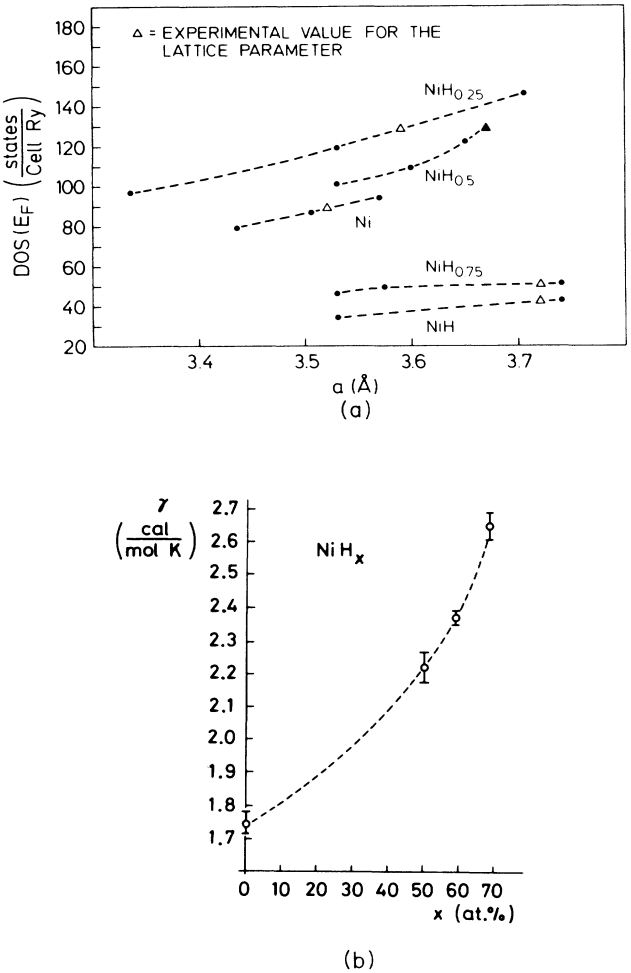

FIG. 10. (a) DOS at the Fermi level (E_F) for the different stoichiometric, ordered NiH systems; the black points represent the calculations at different volumes; the triangle represents the DOS value at the experimental equilibrium volume. (b) Experimental values for the γ coefficient of the electronic specific heat for different nonstoichiometric NiH_x hydrides; the experimental values for γ are taken from Ref. 15.

where λ is the electron-phonon enhancement parameter and k_B is the Boltzmann constant. For pure Ni, at the experimental volume, we obtained $D(E_F)=1.65$ states/(atom eV), which is close to the value of 1.69 calculated in Ref. 12. For $\lambda=0$ this would give the value $\gamma=3.39$ (mJ mol^{-1} K^{-2}). Experimental values for γ ranging from 5.23 to 7.28 mJ mol^{-1} K^{-2} have been reported.[13,14] This indicates a larger value for the enhancement parameter λ varying between 0.54 and 1.15. Our results for $D(E_F)$ values at the experimental volumes for the various hydrides indicate an increase of the γ coefficient with H concentration up to $x=0.5$. For $NiH_{0.75}$ and NiH, $D(E_F)$ is smaller than the value for pure Ni. This suggests that the γ coefficient should also be lower than in pure Ni. Assuming the same λ value for the NiH_x hydrides as for pure Ni, we obtain for $x=0.25$ and 0.5 larger γ values than the observed. However, we recall that the experimental curve in Fig. 10 was derived from experimental γ values for nonstoichiometric Ni hydrides where the two phases of Ni (para- and ferromagnetic) were simultaneously present in the sample.[15]

IV. MAGNETIZATION

The ferromagnetic properties of Ni (bulk[16] and surface[17]) are strongly affected by the presence of interstitial H atoms. The average saturation magnetization of different Ni hydrides shows a continuous dimunition by increasing H concentration. NiH_x systems with more than 65 at. % hydrogen are paramagnetic. Experimental results are shown in Fig. 11(b), in which two phases of NiH_z were present (para- and ferromagnetic). Our spin-polarized band-structure calculations in pure Ni, $NiH_{0.25}$, and $NiH_{0.50}$ also show a decreasing of the saturation magnetization by increasing the H content. The measured initial decrease of the magnetic moment per added H atom in Ni is $0.8\mu_B$, which can be deduced from the experimental curve in Fig. 11(a). Our theoretical result is a dimunition of $(0.65\pm0.05)\mu_B$ in the average magnetic moment of Ni per H atom. This close agreement between the experimental results for the magnetization of a two-phase hydride with our results for a single, ordered phase may at first seem surprising, but it simply reflects the fact that the effects of H in Ni are very localized (see Sec. III). In Table II we show the theoretical results for the charge and

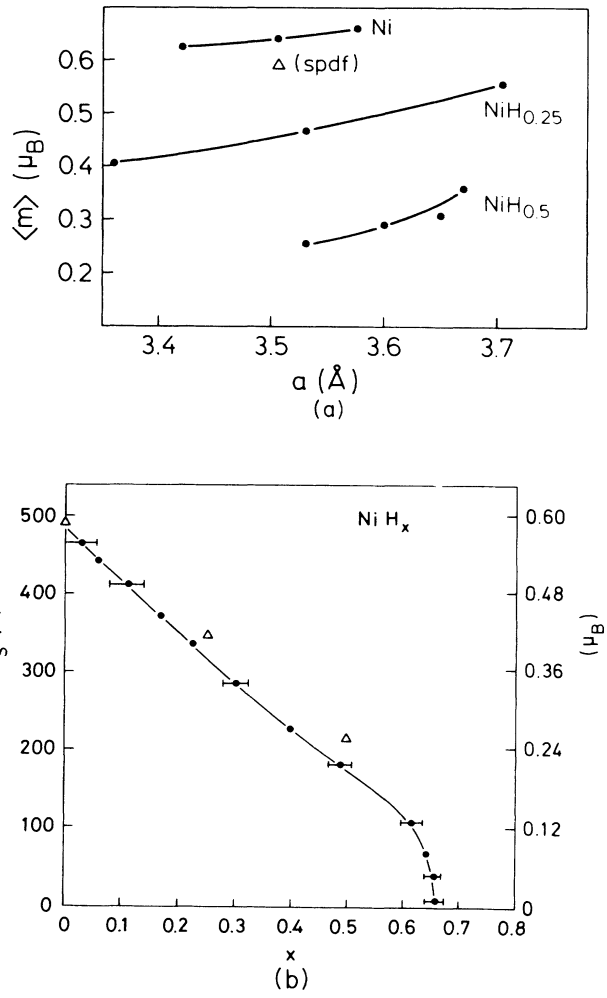

FIG. 11. (a) Theoretical value of the average magnetization per Ni atom in the different ferromagnetic Ni_x hydrides. The black points represent the theoretical values at different volumes. The triangles represent a theoretical calculation for pure nickel in which f partial waves have been included. (b) Experimental curve for the saturation magnetization in Ni_x hydrides as a function of the H concentration (Ref. 16). The triangles represent our theoretical predictions.

TABLE II. Total charge n (in $|e|$) and magnetization m (Bohr magnetons μ_B) in each atomic sphere (see Fig. 1). The difference volumes for Ni, $NiH_{0.25}$, $NiH_{0.5}$, $NiH_{0.75}$, and NiH correspond to $a=3.505$, 3.53, 3.651, 3.741, and 3.741 Å, respectively.

	Ni		$NiH_{0.25}$		$NiH_{0.5}$		$NiH_{0.75}$	NiH
Sphere	n	m	n	m	n	m	n	n
1	0.150	0.646	0.200	0.7440	−0.03	0.45	−0.503	−0.481
2	0.150	0.646	−0.069	0.3805	−0.03	0.45	−0.262	−0.481
3	0.150	0.646	−0.069	0.3805	−0.30	0.17	−0.262	−0.481
4	0.150	0.646	−0.069	0.3805	−0.30	0.17	−0.262	−0.481
5	−0.150	−0.0045	−0.153	−0.0036	−0.14	−0.0025	0.476	0.481
6	−0.150	−0.0045	−0.153	−0.0036	−0.14	−0.0025	0.476	0.481
7	−0.150	−0.0045	−0.153	−0.0036	0.47	−0.0042	0.476	0.481
8	−0.150	−0.0045	0.466	−0.0040	0.47	−0.0042	−0.139	0.481

magnetic moment inside each atomic sphere in the unit cell for pure Ni, $NiH_{0.25}$, and $NiH_{0.5}$ at the corresponding experimental volumes.

Figure 12 shows the spin density and the total density inside the H sphere in the $NiH_{0.25}$ system. In the upper panel the total charge density around the proton in the octahedral site and the total charge for an isolated H atom are shown. In all hydrides we found an enhancement of the total charge density around the proton which is larger than just the sum of the interstitial charge density without H plus the charge density of an isolated H atom. Thus, the proton in Ni is "overscreened" by the conduction electrons; the hydrogen is more electronegative than Ni. In the case of the ferromagnetic systems, we found also an enhancement for the spin polarization at the proton site as shown in Fig. (12). At this site the spin polarization is directed opposite to the bulk magnetization but very small (of the order of $10^{-3}\mu_B$, see Table II). From the value for the spin density at the proton site we estimated the hyperfine field. If the interaction between nuclear spins and electron orbital current is neglected and, for a site with cubic symmetry, the hyperfine field $H_{\rm hf}$ at a site of cubic symmetric environment is given by[18]

$$H_{\rm hf}=\tfrac{8}{3}\pi\mu_B\int^{\varepsilon_F}d\varepsilon[\rho_\uparrow(0,\varepsilon)-\rho_\downarrow(0,\varepsilon)]\,,$$
$$=\tfrac{8}{3}\pi\mu_B\rho_{\rm spin}(0)\,, \tag{6}$$

where $\rho_{\rm spin}(0)$ is the spin density at the nucleus ($r=0$). Its value at the proton site at the experimental volume in

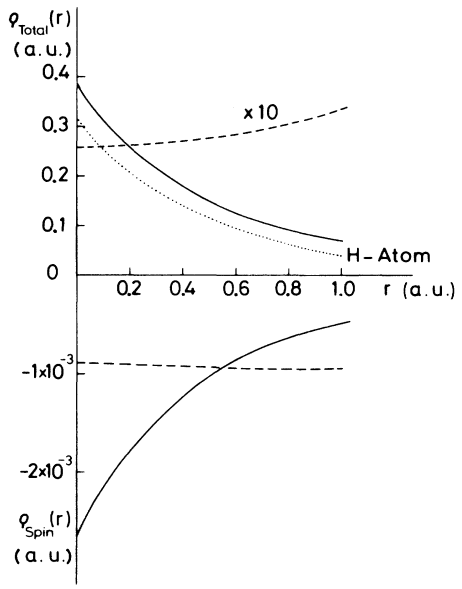

FIG. 12. Spherically averaged total electron density inside the atomic H sphere in $NiH_{0.25}$ (solid line). The electron density for the interstitial sphere is also indicated (dashed line). The dotted line indicates the total electron density for the free H atom in the ground state (i.e., the $1s$ electron density). The lower panel shows the spin density (spherical average) around the proton site in $NiH_{0.25}$ (solid line). The negative values indicate that the polarization cloud around the proton has the opposite direction from the bulk magnetization. The dashed curve shows the polarization in the empty interstitial sphere.

$NiH_{0.25}$ is $\rho_{\rm spin}(0)=-0.0028$ a.u.$^{-3}$ (see Fig 12), giving the value $H_{\rm hf}=-1.51$ kG. This value may be compared with the experimental result,[19] -0.64 kG, obtained for positive muons in Ni, in μSR experiments at low temperatures. However, the zero-point motion of the muon around its equilibrium position reduces the hyperfine field, and also the lattice relaxation around the impurity for very low concentrations may affect this field (see Sec. VI).

V. CHARGE TRANSFER

In spite of the approximate nature of our charge calculations,[20] we may try to deduce some charge-transfer trends. Due to the screening of the proton in the interstitial sites in Ni by the conduction electrons, there is an electron transfer between the Ni atoms and H atoms. The calculated total radial electronic charge in each atomic sphere shows that the total charge inside a sphere of radius R around the proton located at the octahedral site in Ni is larger than the electronic charge inside the same sphere in the case of the isolated H atom. Table III shows the results for the charge transfer to hydrogen in the different hydrides at given volumes. The theoretical value for the electronic charge Z in the ground state inside of a sphere of radius R in the case of an isolated H atom is given by (in a.u.)

$$Z=1-(1+2R+2R^2)e^{-2R}\,, \tag{7}$$

which is easily found by integration of the $1s$ charge density for the isolated H atom. We shall discuss the charge transfer in more detail in the following section.

VI. DISCUSSION

Concerning the volume change produced by H in transition metals, it is experimentally found[11] that for almost all transition metals the introduction of one H atom produces a volume expansion, $\Delta V_{\rm H}$, of 2.8 Å^3. By rearranging Eq. (4), which is valid for low H concentrations ($x<1$), we get

$$\Omega_{NiH_x}=\Omega_{\rm Ni}+x\Omega_{\rm H}\,. \tag{8}$$

Here, $\Omega_{\rm NiH}$ and $\Omega_{\rm Ni}$ are the atomic volumes of the NiH_x hydride and pure Ni, respectively; Ω_H represents the atom

TABLE III. Total number of electrons Δn inside a sphere of radius R around the proton in the octahedral site in the different Ni hydrides, the third column indicates the number of electrons inside the same spheres in the ground state for the isolated H atom. The last column shows the values for the charge transfer to H, ΔZ (in electrons), according to Mulliken's population analysis (see Sec. VI).

	R (a.u.)	Δn	Δn (free H atom)	ΔZ
$NiH_{0.25}$	1.0553	+0.533	+0.353	0.48
$NiH_{0.5}$	1.0765	+0.528	+0.365	0.46
$NiH_{0.75}$	1.1184	+0.524	+0.387	0.43
NiH	1.1184	+0.519	+0.387	0.43

volume of "metallic hydrogen," $\Omega_H = \Delta V_H$. Equation (8) is also the well-known Vegard's law,[21] which establishes in a first approximation, the atomic volume of an interstitial solid solution of two metals as a weighted sum of the constituent atomic values. It is in this context, also valid for other transition metals M, with the same value for Ω_H and for low H concentrations (i.e., $\Omega_{MH} = \Omega_M + x\Omega_H$). By this way of interpretation H behaves in metals as a metal with an atomic volume of ≈ 3 Å^3. It is interesting to note that the theoretical value for the equilibrium atomic volume of metallic hydrogen, computed[12] in total-energy minimization yields the value of 2.946 Å^3, in agreement with the experimental value for ΔV_H found in many transition metals.

As shown here for the NiH_x compounds, it has been also found for many other transition-metal hydrides that the most important feature in the DOS curves is the change of the density of states below the Fermi energy, corresponding to the appearance of localized H s states.[22] This aspect is qualitatively illustrated in Fig. 3. These low lying-states are a mixing of $4s$, $4p$, and $3d$ Ni states with the $1s$ state of hydrogen. The strong H s—Ni d hybridization in Ni hydrides can be easily understood by looking at the $3d$ levels of atomic Ni (≈ -1.1 Ry),[23] which are very close to the ground-state energy of the H atom. Therefore, a strong mixing is expected between these states, especially in the shell of Ni atoms closest to the H atom, where the $3d$ $1s$ overlap is not negligible. The low-lying states produced by the addition of H in the host metal lattice have also been seen in photoemission experiments.[24] We find two major changes in the DOS below the d bands; two strong peaks appear at 0.3 and 0.6 Ry below the Fermi energy, respectively. The peak at $E_F - 0.3$ Ry is essentially an enhancement of $4p$ and $4s$ levels of Ni, and the lower states at $E_F - 0.6$ Ry have mainly H $1s$ character. Some photoemission measurements[25] from H absorbed on Ni surfaces have shown the existence of a peak at ≈ 0.3 Ry below E_F with sp-like character, produced by enhancement of bulk bands of Ni. The peak at $E_F - 0.6$ Ry below had so far not been detected. Differences in the DOS for Ni-H systems as compared to that of pure Ni cannot be explained within a rigid-band model. However, this model can explain the reduction of the saturation magnetization with increasing H concentration. In the rigid-band approximation each H atom loses its $1s$ electron, the Fermi energy increases with x, and thus the unoccupied part of the Ni d bands is slowly filled and a continuous decrease of the magnetization would occur without changing the DOS of pure Ni. In the past many of the observed properties of metal-hydrogen systems were explained using simplified models for hydrogen in metals, the proton model,[26] and the anion model.[27] The former is related to the rigid-band model. We found the neither the proton—rigid-band model nor the anion model is valid in Ni. This conclusion also holds[24] for H in many other transition metals and transition-metal alloys.

The enhancement of the electronic charge around the proton in the metal is the normal response of an electron gas which tends to screen the positive charge of the proton. This has been demonstrated[28,29] in many types of approaches studying a proton immersed in an electron gas with uniform density (jellium). The screening cloud around the proton is always greater than the electron cloud around the proton in the isolated hydrogen atom. This enhancement is compensated at larger distances by the Friedel oscillations. In our case, inside the atomic sphere containing the proton with a radius of ≈ 1 a.u., we find an electron density shape which is very similar to the atomic $1s$-electron cloud (see Fig. 12). In order to compare the electronic charge inside the atomic sphere for H with other definitions of the charge transfer, we assume that the total electronic charge inside the hydrogen sphere is obtained by integrating an enhanced $1s$ charge density. Comparing this value with the corresponding result for the free H atom, we get the following values (in electrons) for the charge transfer to hydrogen: 0.48 in $NiH_{0.25}$, 0.46 in $NiH_{0.5}$, 0.43 in $NiH_{0.75}$, and 0.43 in NiH. The integrations were performed with the radius for the H sphere as given in Table III. With this definition of charge transfer we can compare the values with the results obtained by means of a Mulliken's population analysis.[30] This is frequently used in cluster calculations using a linear combination of atomic orbitals (LCAO) as basis functions. The value of 0.48 electrons for the charge transfer to H in $NiH_{0.25}$ agrees very well with values obtained for H in clusters of transition metals by using the orbital population analysis.[31,32]

The calculated "static" value of -1.54 kG for the hyperfine field at the proton site in the NiH systems, is considerably larger in magnitude than the experimental value -0.64 kG for a muon in Ni. This can be explained as an effect of the zero-point motion of the point charge around the octahedral site. The amplitude in these oscillations is considerably larger for the muon than for a proton, due to the smaller value of the mass of the muon. Thus, instead of using, in the case of the muon, the value for the spin density at the proton site in Ni hydride, we average the magnetization density over the region covered by the zero-point amplitude around the equilibrium position of the muon in nickel. An estimate of the zero-point amplitude $\langle x^2 \rangle^{1/2}$ for the muon in an octahedral site in Ni may be made by looking at the neutron scattering measurements for the frequencies ω of localized hydrogen in transition metals.[33] We assume a value of $\hbar\omega = 100$ meV for the zero-point energy of a muon in nickel, and within the harmonic-potential approximation, the zero-point amplitude is given by

$$\langle x^2 \rangle^{1/2} = \left[(2n+1) \frac{\hbar}{2m_\mu \omega} \right]^{1/2} . \tag{9}$$

Here m_μ is the muon mass ($\frac{1}{9}$ of proton mass) and we obtain for the ground state ($n=0$) $\langle x^2 \rangle^{1/2} = 0.43$ Å. This indicates that the wave function representing a *muon* as a quantum particle in nickel is localized within a sphere of radius ≈ 1 a.u. around the octahedral site. Therefore, we average the spin density inside the atomic sphere representing the H atom in our calculation. The value obtained is $\bar{\rho} = 2.8 \times 10^{-4}$ a.u., and the corresponding hyperfine field [see Eq. (6)] is -0.44 kG. The magnitude, 0.44 kG, represents a lower theoretical bound for the hyperfine

field of muon in nickel since it has been assumed that the electrons do not follow the movement of the point charge around its equilibrium position. This large reduction of the size of the hyperfine field due to the vibrational motion of the muon around its equilibrium interstitial site has been also found in nonmetallic hosts, like diamond.[34]

Concluding, we summarize the main features of our calculations on stoichiometric NiH systems as follows:

(i) The inclusion of hydrogen in the octahedral interstitial sites in Ni causes an increase of the volume by $\Delta V_H \approx 2.6$ Å^3 per H atom added.

(ii) The ferromagnetic properties of pure Ni change drastically with the addition of H due to the filling of the holes in the minority d bands of Ni. The magnetization reduction is found to be $(0.65\pm0.05)\mu_B$ per added H atom.

(iii) The DOS at the Fermi energy for ferromagnetic $NiH_{0.25}$ and $NiH_{0.5}$ is larger than that of pure Ni. This explains the increase of the γ coefficient of the electronic specific heat of Ni hydrides by increasing H concentration.

(iv) Due to the inclusion of H, the shape of the DOS curve of Ni is strongly changed. Specifically, new low-lying states appear far below the Fermi level as a consequence of hybridization between the s states of hydrogen and the bulk states of Ni. These states, below the Ni $3d$ bands, have also been observed in photoemission experiments. Accordingly the rigid-band model is not applicable for NiH systems.

(v) The electron density around the proton in the octahedral site is strongly enhanced. Inside a sphere of radius ≈ 1 a.u. around the proton there are more electrons than in the case of the free H atom. A charge transfer also occurs from the neighboring Ni atoms to the H atom. The electron density shape around the proton in the bulk is very similar to the $1s$ density. The spin density around the proton is in an opposite direction to the bulk polarization but the magnetization of the H atom is very small ($\approx 10^{-3}$ a.u.).

(vi) The hyperfine field of muon in Ni can be calculated from the "static" values for the spin density around the proton in Ni by using the spin-density average over the region covered by the zero-point motion of the muon.

ACKNOWLEDGMENTS

We are grateful to H. Kronmüller, who encouraged us to perform this analysis, and to O. K. Andersen for helpful discussions.

*Permanent address: Physics Department, USACH, Santiago-2, Chile.

[1]See, e.g., H. Moesta, in *Chemisorption und Ionisation in Metall Systemen* (Springer-Verlag, Berlin, 1968); V. Ponec, Z. Knor, and S. Cerny, *Adsorption in Solids* (Butterworths, London, 1974); Gerd Wedler, *Chemisorption* (Butterworths, London, 1976); A. W. Adamson, *Physical Chemistry of Surfaces* (Wiley, New York, 1982); J. Harris and S. Anderson, Phys. Rev. Lett. **55**, 1583 (1985).

[2]See, e.g., A. Seeger, in Proceedings of the Yamada Conference VIII, Muon Spin Rotation, Shimada 1983, Hyperfine Interactions **17-19**, 75 (1984); K. W. Kehr, in *Hydrogen in Metals I,* edited by G. Alefeld and J. Vökl (Springer-Verlag, Berlin, 1978); J. Völkl and G. Alefeld, *ibid*; D. Emin, M. J. Baskes, and W. D. Wilson, Phys. Rev. Lett. **42**, 791 (1979).

[3]O. K. Andersen, Phys. Rev. B **12**, 3060 (1975).

[4]U. von Barth and L. Hedin, J. Phys. C **5**, 1629 (1972).

[5]See, e.g., E. O. Wollan, J. W. Cable, and W. C. Koehler, J. Phys. Chem. Solids **24**, 1141 (1963); V. F. Petrunin, S. K. Dolukhanyan, M. G. Zemlyanov, S. V. Marchenko, and P. P. Parshin, Fiz. Tverd. Tela (Leningrad) **23**, 1926 (1981) [Sov. Phys.—Solid State **23**, 1126 (1981)]. H. D. Carstenjen, Phys. Status Solidi A **59**, 11 (1980); S. T. Picraux, Nucl. Instrum. Methods **182/183**, 413 (1981); A. L. Companion, F. Liu, and D. P. Onwood, J. Less. Common Met. **107**, 131 (1985).

[6]E. G. Ponyatovskii, V. E. Antonov, and I. T. Belash, Usp Fiz. Nauk **137**, 663 (1982) [Sov. Phys.—Usp. **25**, 596 (1982)].

[7]A. R. Mackintosh and O. K. Andersen, in *Electrons at the Fermi Surface,* edited by M. Springford (Cambridge University Press, Cambridge, England, 1980); D. Glötzel, in *Physics of Solids under High Pressure,* edited by J. S. Schilling and R. N. Shelton (North-Holland, Amsterdam, 1981); R. M. Niemenen and C. H. Hodges, J. Phys. F **6**, 573 (1976).

[8]D. G. Pettifor, Commun. Phys. **1**, 141 (1976).

[9]V. Heine, Solid State Phys. **35**, 1 (1980).

[10]K. A. Gschneider, in *Solid State Physics 16,* edited by F. Seitz and D. Turnbull (Academic, New York, 1964).

[11]See, e.g., H. Peisl, in *Hydrogen in Metals I,* edited by G. Alefeld and J. Völkl (Springer-Verlag, Berlin, 1978).

[12]V. L. Moruzzi, J. F. Janak, and A. R. Williams, *Calculated Electronic Properties of Metals* (Pergamon, New York, 1978).

[13]R. H. Busey and W. F. Giauque, J. Am. Chem. Soc. **74**, 3157 (1952).

[14]J. A. Rayne and N. R. G. Kemp. Philos. Mag. **1**, 918 (1956).

[15]G. Wolf and B. Baranowski, J. Phys. Chem Solids **32**, 1649 (1971).

[16]H. J. Bauer and E. Schmidbauer, Z. Phys. **164**, 367 (1961).

[17]M. Landolt and M. Campagna, Phys. Rev. Lett. **39**, 568 (1977); M. Weinert and J. W. Davenport, Phys. Rev. Lett. **54**, 1547 (1985).

[18]C. P. Slichter, *Principles of Magnetic Resonance* (Springer-Verlag, Berlin, 1978).

[19]K. Nayamine, S. Nagamiyqa, O. Hushimoto, N. Nishida, I. Yamasaki, and B. D. Patterson, Hyperfine Interactions **1**, 577 (1976); M. Cameni, F. N. Gygax, N. Ruegg, A. Schenk, and H. Schilling, Phys. Lett. **60A**, 439 (1977).

[20]The charge values calculated are of course dependent on the actual choice of sphere radius ratios. Thus, our calculated "charge transfers" should not be taken too rigorously.

[21]L. Vegard, Z. Phys. **5**, 17 (1921).

[22]See, e.g., A. C. Switendick, Ber. Bunsenges. Phys. Chem. **76**, 536 (1972); Z. Phys. Chemie (Neue Folge) **117**, 89 (1979); D. A. Papaconstantopoulos, B. M. Klein, E. N. Economu, and L. L. Boyer, Phys. Rev. B **17**, 141 (1978); C. D. Gelatt, H. Ehrenreich, and J. A. Weiss, Phys. Rev. B **17**, 1940 (1978); J. S. Faulkner, Phys. Rev. B **13**, 2391 (1976); H. Katayama, K. Terakura, and J. Kanamori, Solid State Commun. **29**, 431 (1979); C. T. Chan and S. G. Louie, Phys. Rev. B **27**, 3325

(1983); O. Jepsen, R. M. Nieminen, and J. Madsen, Solid State Commun. **34**, 575 (1980); B. M. Klein and W. E. Pickett, J. Less. Common. Met. **103**, 185 (1984); J. K. Nørskow, Phys. Rev. Lett. **48**, 1620 (1982); M. Gupta, Phys. Rev. B **25**, 1027 (1982); D. J. Peterman, D. K. Misemer, J. H. Neaver, and D. T. Peterson, *ibid.* **27**, 799 (1982); M. Gupta and A. J. Freeman, *ibid.* **17**, 3029 (1978); A. Fujimori and N. Suda, Solid State Commun. **41**, 491 (1982); A. R. Williams, J. Kübler, and C. D. Gelatt, Jr., Phys. Rev. B **19**, 6094 (1979); M. Methfessel and J. Kübler, J. Phys. F. **12**, 141 (1982); K. M. Ito, H. J. Tao, and X. Y. Zhu, Phys. Rev. Lett. **53**, 1586 (1984).

[23]F. Hermann and S. Skillman, *Atomic Structure Calculations* (Prentice-Hall, Englewood Cliffs, 1963).

[24]See, e.g., D. J. Peterman, D. K. Misemer, J. H. Neaver, and D. T. Peterson, Phys. Rev. B **27**, 799 (1982); R. P. Messmer, D. R. Salahub, K. H. Johnson, and C. Y. Yang, Chem. Phys. Lett. **51**, 84 (1977); K. Tanaka, N. Hamasaka, M. Yasuda, and Y. Fukai, Trans. J. Inst. Met. Suppl. **21**, 65 (1980); J. H. Weaver, D. J. Peterman, D. T. Peterson, and A. Franciosi, Phys. Rev. B **23**, 1692 (1981); Y. Fukai, S. Kazama, K. Tanaka, and M. Matsumoto, Solid State. Commun. **19**, 507 (1976); D. E. Eastman, J. K. Cashion, and A. C. Switendick, Phys. Rev. Lett. **27**, 35 (1971); T. Riesterer, J. Osterwalder, and L. Schlapbach, Phys. Rev. B **32**, 8405 (1985); F. Greuter, I. Strathy, and E. W. Plummer, *ibid.* **33**, 736 (1986).

[25]F. J. Himpsel, J. A. Knapp, and D. E. Eastman, Phys. Rev. B **19**, 2872 (1979).

[26]See, e.g., I. Isenberg, Phys. Rev. **79**, 736 (1950); N. F. Mott and H. Jones, *Theory of the Properties of Metals and Alloys* (Oxford University Press, London, 1958).

[27]See, e.g., C. E. Messer, J. Solid State Chem. **2**, 144 (1970); G. G. Libowitz, in *The Solid State Chemistry of Binary Metal Hydrides* (Benjamin, New York, 1965).

[28]C. O. Almbladh, U. von Barth, Z. D. Popovic, and M. J. Stott, Phys. Rev. B **14**, 2250 (1976).

[29]J. Gondzik and H. Stachowiak, J. Phys. C **18**, 5399 (1985).

[30]R. S. Mulliken, J. Chem. Phys. **2**, 782 (1934).

[31]H. Adashi and S. Imoto, J. Phys. Soc. Jpn. **46**, 1194 (1979).

[32]P. Vargas, H. Kronmüller, and M. C. Böhm, Z. Phys. Chem. **143**, 229 (1985).

[33]W. Kress, in *Landolt-Börnstein Tables (New Series)*, edited by K. H. Hellwege (Springer-Verlag, Berlin, 1983), Band 13b.

[34]N. Sahoo, S. K. Mishra, K. C. Mishra, A. Coker, T. P. Das, C. K. Mitra, L. C. Snyder, and A. Glodenu, Phys. Rev. Lett. **50**, 913 (1983).